HHS Public Access

Author manuscript

Int J Pharm. Author manuscript; available in PMC 2021 June 30.

Published in final edited form as:

Int J Pharm. 2020 June 30; 584: 119438. doi:10.1016/j.ijpharm.2020.119438.

MODIFIED ELECTROSPUN CHITOSAN MEMBRANES FOR CONTROLLED RELEASE OF SIMVASTATIN

Vishnu Priya Murali[a,*,i], **Tomoko Fujiwara**[b], **Caleb Gallop**[b], **Yongmei Wang**[b], **Jack A. Wilson**[a], **Matthew Thomas Atwill**[a], **Mallesh Kurakula**[a], **Joel D. Bumgardner**[a]

[a]Department of Biomedical Engineering, University of Memphis, Memphis, TN 38152, USA

[b]Department of Chemistry, University of Memphis, Memphis, TN 38152, USA

Abstract

Chitosan nanofibrous membranes have immense potential in tissue engineering and drug delivery applications because of their high degree of biocompatibility, their ability to mimic the extracellular matrix and increased surface area. However, their use is often limited due to their extreme hydrophilic nature causing them to lose their nanofibrous structure. In this study, chitosan membranes were modified either by acylation reactions using fatty acids of different chain lengths or tert-butyloxycarbonyl (tBOC) protecting groups to increase the hydrophobicity of the membranes and protect the nanofibrous structure. The modified membranes were characterized using scanning electron microscopy, attenuated total reflectance Fourier transform infrared spectroscopy, water contact angle and elemental analysis to confirm the addition of the modification groups. These membranes were then evaluated to control the release of a hydrophobic osteogenic drug-simvastatin (SMV). The interaction between SMV and the polymer were determined using molecular modeling. SMV and SMV loaded membranes were further tested for their *in vitro* cytotoxicity and osteogenic potential. Results showed that as the fatty acid chain length increased from two to six methylene groups, the hydrophobicity of the membranes increased (59.2±8.2° to 94.3±8.5°water contact angle). The amount of drug released from the membranes could be controlled by changing the amount of initial drug loading and the type of modifications. For a 500μg loading, after 4 weeks, the short chain fatty acid modified membranes released 17.8 ± 3.2% of the drug whereas a long chain fatty acid released only 4.8±0.8%. On the

[*]Corresponding author: vmurali@memphis.edu.

[i]Present address: Department of Chemical & Biomedical Engineering, Florida State University, Dittmer Chemistry, 95 Chieftan Way, Tallahassee, FL- 32306, USA

CRediT Roles

Vishnu Priya Murali: Methodology, Validation, Formal analysis, Investigation, Data curation, Writing-Original draft, Visualization
Tomoko Fujiwara: Conceptualization, Formal analysis, Methodology, Resources, Writing- review & editing
Caleb Gallop: Formal analysis, Methodology, Data curation, Software, Writing- review & editing
Yongmei Wang: Validation, Methodology, Resources, Writing- review & editing
Jack Wilson & Matthew Thomas Atwill: Investigation, Validation
Mallesh Kurakula: Investigation, Formal analysis
Joel Bumgardner: Conceptualization, Resources, Writing- review & editing, Supervision, Project administration, Funding acquisition

Declaration of Competing Interest

The authors declare no competing financial interest

other hand, for a 50μg loading, short chain modified membranes released 73.3 ±33.3% of the loaded drug and the long chain membranes released 43±3.5%. The long chain fatty acid membranes released SMV for extended time periods of up to 90 days. This data was further supported by molecular modeling, which showed that SMV was more compatible with more hydrophobic membranes. Cell studies showed that SMV from 75 to 600ng/ml range possessed osteogenic potential in a dose dependent manner and the amount of SMV released from the most hydrophobic FA treated membranes was not cytotoxic and supported osteogenic differentiation. This study demonstrates our ability to control the release of a hydrophobic drug from chitosan membranes based on the clinical need.

Graphical Abstract

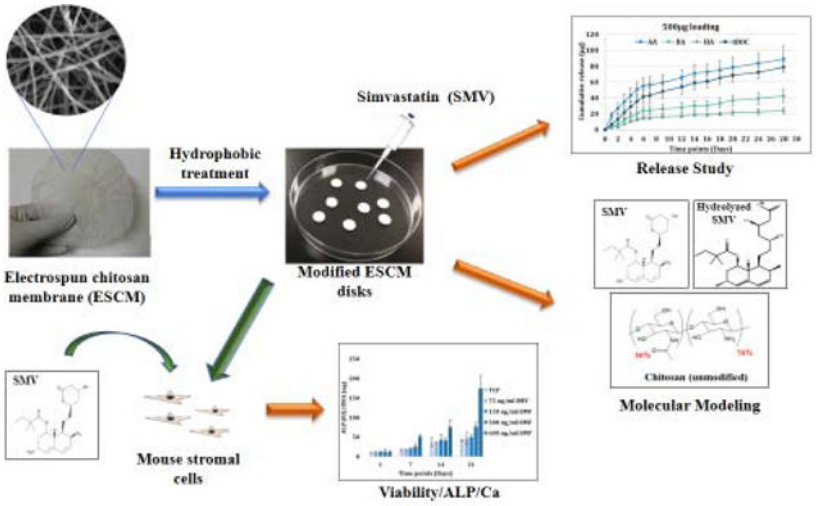

Keywords

Chitosan; Electrospun membranes; Simvastatin; Controlled release; Osteogenesis

1. Introduction

Chitosan, derived from a natural polymer, chitin, is a linear chain polysaccharide made of N-acetyl glucosamine and glucosamine units. Chitosan has been investigated for a wide range of biomedical applications due to its excellent biocompatibility, controllable degradation and ability to be manufactured into various forms like films, beads, hydrogels, sponges and particles, to name a few [1–4]. Chitosan can be electrospun to produce membranes with fiber diameters in the nano-scale range that mimic the nanofibrous structure of the natural extracellular matrix (ECM) [5]. The ability to mimic the natural nanofibrous structure of the ECM is advantageous for supporting growth and proliferation of cells important to tissue engineering/regeneration strategies [5–7]. Another advantage of the nanofibers created by the electrospinning process is the increased surface area for loading and delivering therapeutic agents [8–10]. Because of this combination of degradability and nanofiber structure, electrospun chitosan membranes (ESCM) are investigated for a number of tissue

regeneration and drug eluting tissue scaffold applications including dental and orthopedic [1, 2, 7, 11–17].

Trifluoroacetic acid (TFA) is one of the most commonly used solvent for electrospinning chitosan as it provides adequate viscosity for the polymer solution to be pulled into nanofibers [18, 19]. However, TFA forms a salt with the amino groups on the chitosan polymer during the spinning process and must be removed. Two strategies have been developed to remove the salts without compromising the nanofiber structure or deteriorating the mechanical properties of the ESCM (13,22). One of the techniques involves a Triethylamine (TEA) wash to remove the TFA ions, followed by blocking of chitosan's amino groups on the surface of the fibers with tBOC groups (di tert butyl dicarbonate) to prevent amine protonation that can lead to swelling in aqueous environments [17]. Another technique developed by Wu et al. involves grafting fatty acid (FA) groups to the hydroxyl groups on the outside of the chitosan fibers to create a hydrophobic wrap that would prevent fiber swelling during water rinsing steps to remove the TFA ions [20]. The fatty acids can be subsequently removed with alkali, as desired, to regenerate the native ESCM [20]. The TEA/tBOC and the FA-modified chitosan membranes demonstrated the ability to maintain the nanofibrous structure in aqueous environments as compared to alkali based treatments used to remove TFA salts, while maintaining good mechanical, degradation and cytocompatibility properties [17, 20]. Both types of membranes have shown promise for regenerating bone in guided bone regeneration (GBR) applications in rodent models [17, 20, 21].

While GBR membranes have been made bioactive through the addition of therapeutics such as bone morphogenetic protein-2 (BMP-2) to augment healing of bone grafted sites, dosing and release profiles of BMP-2 are not optimal and have been implicated in adverse reactions such as ectopic bone formation, bone/tooth root resorption and ankylosis [22, 23]. These are also associated with high therapeutic costs [22, 23]. To circumvent these drawbacks, we propose to locally deliver a drug called simvastatin (SMV), which has recently been reported to possess good osteogenic property [24–29]. This drug belongs to the statin class of pharmaceuticals and is used in clinics for anti-cholesterol treatment. SMV has been reported to promote bone growth and healing after local delivery, by antagonizing TNF-α inhibition of BMPs, decreasing osteoclast activity and improving angiogenesis [30–33]. Studies also reported a positive association between statin use by elderly patients and reduction in the risk of hip fracture [34, 35]. SMV has shown to induce osteogenic differentiation of bone marrow stromal cells, increasing the alkaline phosphatase (ALP) activity and osteocalcin (OCN) and osteopontin production [26, 36, 37] *in vitro* and better bone healing *in vivo* [38, 39]. SMV is also reported to possess anti-inflammatory and anti-microbial properties that may play a critical role in the tissue regeneration process [31, 40].

This study investigated the potential of adding SMV to tBOC or FA-modified chitosan membranes for the purpose of increasing bioactivity of chitosan GBR membranes for bone regeneration. The modified membranes were characterized for morphology, degree of modification (DM) and hydrophobic behavior. This study examined effects of different levels of loading and membrane modifications for controlling release of SMV from the membranes. Molecular modeling was used to evaluate the interaction between the differently modified chitosans and SMV to understand the mechanism of drug release. Different

concentrations of SMV were tested on mouse stromal cells to identify effects of dosing on ALP production and *in vitro* mineralization. Further, cytocompatibility of SMV loaded membranes was evaluated and membranes releasing non-toxic levels of SMV were tested for their osteogenic potential *in vitro*.

2. Materials & Methods

2.1. Materials

Chitosan with 71% DDA and 311 kDa was purchased from Primex. TFA, dicholoromethane (DCM), pyridine, FAs, tetrahydrofuran (THF), TEA, acetone, tBOC were bought from Sigma and Fisher. SMV was purchased from Cayman Chemicals. Reagents for HPLC were HPLC grade and bought from Fisher. W-20-17 cells were obtained from ATCC and cultured as per ATCC instructions. Reagents for cell culture were bought from Fisher. BMP-2 was purchased from GoldBio.

2.2. Electrospinning

Chitosan membranes were fabricated by electrospinning in an in-house spinning setup, as described previously [2, 11, 17, 20]. Briefly, a 5.5% (w/v) chitosan (71% DDA, MW: 311.7kDa) solution was made in 70% TFA and 30% DCM, loaded in a 10 ml syringe with a 20-gauge blunt needle and electrospun at 27 kV using a syringe pump onto an aluminum foil covered collector plate rotating at ~ 8.4 rpm. To ensure better handle ability, each membrane was made with either 10- or 30-ml solution (three 10ml volumes of chitosan solution spun consecutively) to produce 13cm diameter membranes approximately 0.3 ± 0.1 mm or 0.7 ± 0.1 mm thick, respectively. The electrospinning apparatus was housed inside a ventilated box which was vented to the fume hood. The apparatus was operated at room temperature and at 40 to 60% humidity.

2.3. Post-spinning treatment

The ESCMs were treated to remove TFA salts using the TEA/tBOC or FA methods as previously described [17, 20]. Briefly, for the TEA/tBOC treatment, membranes were immersed in 10% (v/v) TEA/acetone solution for 24 hours under mild stirring, washed twice with acetone, and then placed in a tBOC/THF (0.1g/ml) solution for 48hours at 60°C under mild stirring. After 48 hours, membranes were washed three times with acetone and then dried between nylon meshes and paper towels [17]. Once the membranes were dry, they were punched into small 1cm diameter discs and used for experiments.

For the FA treatment, as spun membranes were first punched into 1cm diameter discs and soaked in a pyridine-fatty acid anhydride (v/v) (50–50) solution at 5mg/ml for 1.5 hours. Next, the membranes were washed by gentle stirring in 1L MQ water (18MΩ@25°, Integral 15, Millipore) for 72 hours to remove the unreacted and excess reagents. The water was changed every 24 hours for 3 days, after which the membranes were lyophilized. The FAs used in this study are acetic (AA), butyric (BA) and hexanoic (HA) anhydride. These FAs were chosen based on a previous study where BA (number of methylene groups in the fatty acid chain, n=4) modified chitosan membranes showed good cell attachment and GBR

potential [20, 21]. Here, a slightly smaller (AA; n=2) and slightly longer (HA; n=6) chain fatty acids were evaluated not to significantly affect the biocompatibility of the membranes.

2.4. Scanning Electron Microscopy (SEM)

Membranes were examined under SEM (Nova NANOSEM 650 FEI™) before and after the TEA/tBOC and fatty acid treatments to determine the effects on fiber size and morphology. Three samples of as spun and treated membranes from three different ESCM were examined at four different regions. Parameters used for the measurement were 5000X magnification, 5kV and a spot size of 3.0.

2.5. ATR-FTIR

ATR spectra were collected to evaluate the extent of TFA salt removal by the treatments and attachment of tBOC and FA groups to the chitosan polymer chain. The spectra were collected using FT-IR spectrometer, Frontier (Perkin-Elmer). Three samples of as spun and treated membranes were scanned from 500cm^{-1} to 4000cm^{-1} for 16 times.

2.6. Water contact angle measurement

Water contact angles of modified chitosans (membranes) were determined using a VCA optima measurement machine (AST products, INC, USA). 5μL of water droplets were placed carefully onto the membrane surfaces, and the photographs of the droplets were recorded by a digital camera, after approximately one minute. The contact angles were calculated by the goniometry software of VCA OptimaXE. For each modification, four different membranes were tested at three different regions.

2.7. Elemental analysis

Elemental analysis was carried out to evaluate the extent of modification of the membrane by the tBOC or FA molecules based on the carbon to nitrogen ratio (C/N). C/N of the chitosan would change with modification since the modifying groups will add more carbon to the polymer. The analysis was carried out by Atlantic Microlabs, (Norcross, GA, USA) using Perkin-Elmer Model 2400 series II autoanalyzer. The samples were also analyzed to detect any residual amount of TFA salts left after the treatments. Each sample was vacuum dried and analyzed in duplicates.

The actual C/N number ratio of original chitosan used in this study was calculated by the atomic weight % obtained by elemental analysis, using the following equation:

$$\frac{n_0(C)}{n_0(N)} = \frac{C\%/12.011}{N\%/14.0067} = \frac{6.68}{1} \quad (1)$$

The degree of modification (DM), x is defined as the number of tBOC or FA group per chitosan/chitin monomer unit, and calculated using the atomic weight % of modified chitosan obtained from elemental analysis by the following equation:

$$\frac{n_m(C)}{n_m(N)} = \frac{C\%/12.011}{N\%/14.0067} = \frac{6.68 + px}{1} \quad (2)$$

where C% and N% are weight percentage of carbon and nitrogen, and p is the number of carbon atoms in the substituted groups (specifically, p value for tBOC, acetyl, butyryl, and hexanoyl groups is 5, 2, 4, and 6, respectively).

2.8. *In vitro* SMV loading & release study

SMV release study was performed using 1 cm discs of the TEA/tBOC-, AA-, BA- and HA-modified membranes and each was tested at two different thicknesses; a thin (~0.3mm thick) or thick (~0.7mm) membrane thickness. Four different amounts of SMV- 500, 250, 100, 50μg - were loaded onto the membranes. These amounts were chosen as representative of the wide range of concentrations tested in previous studies which showed significant osteogenic potential [28, 41–43]. SMV at 500 and 250μg, 100 and 50μg were used as representative for high and low dose, respectively. Membranes were disinfected by rinsing in 70% ethanol and drying under UV light for one hour. Since SMV is insoluble in aqueous solvents, stock of SMV solution was made in 200 proof ethanol (non-denatured). To load the membranes, stock solutions were aseptically pipetted on to individual membranes to provide 50, 100, 250 or 500μg SMV per membrane. The volume of SMV stock added onto the membranes was kept to a minimum to ensure complete absorption by the membranes. Membranes were placed in a laminar flow for 20 to 30 minutes to evaporate away the ethanol before placing them in 48-well plates and adding 0.5 ml of PBS. PBS was replaced every day for the first week and then every other day till day 28. The study was continued till day 91, with samples being collected weekly after 28 days. The collected samples were stored at −20°C for further analysis. There were 6 membranes/treatment/thickness/loading amount. An isocratic HPLC method was used to analyze the amount of SMV released from the membranes. SMV was detected at 236 nm using a UV-VIS detector, a solvent phase of 0.1% TFA: acetonitrile (30:70) and injected at a flow rate of 1ml/min [44]. The amount of sample injected was 10μl and was detected using a Hypersil GOLD column (dim-150 X 4.6mm) with a particle size of 5μm (ThermoScientific™), heated to 30°C. Since SMV is insoluble in aqueous solvents, standards were made in PBS-ethanol (50–50) solutions. To maintain consistency between samples and standards, the samples were also diluted with ethanol that was spiked with SMV. The spike SMV was added to compensate for any drug loss during dilution, which might result in negative values. SMV readily hydrolyzes when in aqueous environment, giving rise to three separate HPLC peaks for SMV hydroxy-acid form, lactone form, and dimer form. Area under these three peaks were added and used to calculate the total concentration of SMV in the eluates.

2.9. Computation of Hansen solubility and Flory-Huggins parameter ($X_{1,2}$) of SMV with chitosan and differently modified chitosan

The solubility parameter (δ_T), first suggested by Hildebrand, is defined as square-root of the cohesive energy density (3), where the cohesive energy $E_{coh} = \Delta H_{vap} - RT$, V_m is the molar volume of the substance, and ΔH_{vap} is the heat of vaporization. Hildebrand predicted that non-polar substances with similar solubility parameters, $\Delta\delta_T = |\delta_{T2} - \delta_{T1}| \approx 0$, are generally

more miscible with each other. Hansen proposed splitting the solubility parameter into three components to improve miscibility predictions for a wider range of substances. These three parameters, referred to as Hansen solubility parameters (HSPs), account for dispersion forces (δ_D), dipolar intermolecular forces (δ_P) and hydrogen bonding (δ_H) [45].The sum of these squared parameters is the squared total solubility parameter δ_T (4).

$$\delta_T{}^2 = \sqrt{\frac{E_{coh}}{V_m}} \tag{3}$$

$$\delta_T{}^2 = \delta_D{}^2 + \delta_P{}^2 + \delta_H{}^2 \tag{4}$$

The solubility parameters for any two chemical species (i.e., drug and polymer) can be used to calculate the Flory-Huggins interaction parameter ($\chi_{1,2}$) according to Equation 5, where $V_{m,1}$ is the molar volume of the drug, R is the ideal gas constant and T is the absolute temperature [45]. The subscripts 1 and 2 represent the drug and polymer, respectively. It is interpreted that the drug is more compatible with a polymer for lower values of $\chi_{1,2}$. The interaction parameter $\chi_{1,2}$ decreases as the difference between two solubility parameters $\Delta\delta_T$ decreases. Therefore, lower values of $\Delta\delta_T$ make the drug more compatible with the polymer.

$$\chi_{1,2} = \frac{V_{m,1}}{RT}(\delta_{T2} - \delta_{T1})^2 = \frac{V_{m,1}}{RT}\,\Delta\,\delta_T{}^2 \tag{5}$$

However, chitosan is far from non-polar and $\Delta\delta_T{}^2$ is not the best descriptor for drug-polymer incompatibility. Hansen proposed using $A_{1,2}$ (6) in place of $\Delta\delta_T{}^2$, which was generally found to provide more accurate predictions of $\chi_{1,2}$ for a wider range of systems [45]. The value $A_{1,2}$ is the sum of squared differences of each parameter with weights of $\frac{1}{4}$ applied on the polar and hydrogen bond parameters. By using $A_{1,2}$ in place of $\Delta\delta_T{}^2$, Equation 4 can be rewritten as Equation 6. Therefore, the Flory-Interaction parameter between SMV and chitosan polymer is calculated using Equation 7 [45].

$$A_{1,2} = (\delta_{D2} - \delta_{D1})^2 + \frac{1}{4}(\delta_{P2} - \delta_{P1})^2 + \frac{1}{4}(\delta_{H2} - \delta_{H1})^2 \tag{6}$$

$$\chi_{1,2} = \frac{V_{m,1}}{RT}A_{1,2} \tag{7}$$

The Hansen Solubility Parameters (HSPs) were calculated using Hansen Solubility Parameters in Practice (HSPiP) software version 5.1.08. The SMILES (Simplified Molecular Input Line Entry Syntax) representations of each compound are used as inputs. For the monomeric units of chitosan, the polymer format for SMILES was used. The software predicts the HSPs parameters using group contribution method based on Yamamoto-molecular break method (Y-MB) that splits the input structure to functional groups.

Furthermore, the HSPs for chitosan, AA-chitosan, BA-chitosan, HA-chitosan and tBOC-chitosan were estimated by taking weighted root-mean-squares of the HSPs for N-acetylglucosamine (D, NAc) and glucosamine (D, Glu) monomeric units (Equations 8a,b,c,d) with their respective modifications. The weights are 0.3 for N-acetylglucosamine and 0.7 for glucosamine monomeric units since chitosan with ~70% DDA is used in this work. The weighted averages were taken this way to ensure that the squared sum of the HSPs always equals the squared total solubility parameter as shown in Equation 8d.

$$\delta_{D2} = \left(0.3 \cdot \delta_{D,NAc}{}^2 + 0.7 \cdot \delta_{D,Glu}{}^2\right)^{1/2} \quad (8a)$$

$$\delta_{P2} = \left(0.3 \cdot \delta_{P,NAc}{}^2 + 0.7 \cdot \delta_{P,Glu}{}^2\right)^{1/2} \quad (8b)$$

$$\delta_{H2} = \left(0.3 \cdot \delta_{H,NAc}{}^2 + 0.7 \cdot \delta_{H,Glu}{}^2\right)^{1/2} \quad (8c)$$

$$\delta_{T2}{}^2 = \delta_{D2}{}^2 + \delta_{H2}{}^2 + \delta_{H2}{}^2 = 0.3 \cdot \delta_{T,NAc}{}^2 + 0.7 \cdot \delta_{T,Glu}{}^2 \quad (8d)$$

2.10. Cell culture

W-20-17, ((W-20 clone 17] (ATCC® CRL-2623™)), preosteoblast mouse bone marrow stromal cells, were grown and maintained in Dulbecco's Modified Eagle medium (DMEM) supplemented with 10% FBS and 50μg of penicillin, 50μg of streptomycin, and 100μg of neomycin (PSN) (Gibco™, Molecular Probes™). Cells were cultured in T75 flasks (Nunc™ EasyFlask™, vented) and placed in an incubator supplied with 5% CO_2 at 37°C. The culture medium was changed once in every two days and the cells were sub-cultured when the flask reached 80–90% confluency. Cells used for cell culture experiments were between passage number 4 and 7.

2.11. Cell viability

Cells were seeded in 96 well plates at 1×104 cells/well and allowed to attach overnight. On following day, media containing different concentrations of SMV were added to the well plates, and the drug toxicity was measured after 24 and 72 hours.

Toxicity of membranes with and without SMV loading were evaluated by non-contact culture, using Falcon™ cell culture inserts (0.45 μm pore size PET membrane, 24 well format). Cells were seeded in 24 well plates at 5×104 cells/well and allowed to attach overnight. Following day, cell inserts containing non-loaded and SMV loaded membranes were placed in the well plates. AA and HA membranes loaded with 0 (AA0 & HA0) and 50 (AA50 & HA50) μg SMV were evaluated for membrane toxicity. Since AA and tBOC membranes had similar release profile, AA membranes were used as representative membranes. Similarly, since HA and BA membranes had similar release profile, only HA membrane was used. Relatively low amount of SMV was added to the membranes to avoid

any toxicity to the cells due to higher drug doses. After 1, 3, and 7 days, membrane toxicity was analyzed.

Each drug concentration and membrane were tested in quadruplicates. Cells grown in medium with no drug or membrane was used as control. The toxicity was determined by measuring cell viability using CellTiter-Glo® Luminescent Cell Viability Assay (Promega Corporation) according to manufacturer's protocol.

2.12. Cell mineralization studies

Cells were seeded in 48 well plates at 1×104 cells/well with complete DMEM (DMEM supplemented with 10% FBS and 1% PSN) and left to attach overnight. Next day, complete medium was replaced either with osteogenic medium (complete DMEM supplemented with 5mM beta-glycerophosphate and 50μg/ml ascorbic acid) and non-toxic concentrations of SMV (referred hereafter as regular media) or osteogenic medium with 25ng/ml BMP-2 (BMP-2 medium) and non-toxic concentrations of SMV. To examine the potential interactions between SMV and BMP-2, SMV media were spiked with 25ng/ml BMP-2. The concentrations of SMV added to the medium were 75–600ng/ml. To evaluate the osteogenic potential of SMV loaded membranes, cells were seeded in 24 well plates at 1×105 cells/well and left to attach overnight. On the next day, cell inserts containing non-loaded and drug loaded membranes were placed in the 24 well plates with either regular medium or BMP-2 medium. The cell culture media were completely replenished every two days. After 1, 7, 14 and 21 days, the media were removed, and the cells were lysed by adding 300μl of molecular grade water to each well and freeze-thawing the plates three times. The cell lysates were used to measure double stranded DNA and ALP activity of the cells. Double stranded DNA was measured using a Quant-iT PicoGreen assay kit, from Invitrogen and the ALP activity was measured using a QuantiChromTM alkaline phosphatase assay kit (DALP-250) from BioAssay Systems. The activity of cells was then normalized to double stranded DNA (dsDNA) (ng/ml) and expressed as IU/ng DNA. Additional plates were made for day 14 and 21 to carry out calcium deposition assay. After the designated time points, medium was completely removed from the wells and the cell layers were carefully washed twice with 500μl of warm PBS. To each well, 500μl of 0.5N acetic acid was added and the plates were placed on a rotary shaker (Belly Dancer™, Strovall, life science Inc., Greensboro, NC, USA) at moderate speed for 24 hours to solubilize the deposited calcium. Next day, the entire well content was transferred to labelled microcentrifuge tubes and frozen at −20°C until ready to assay. A calcium reagent set (Pointe Scientific, Inc), based on o-cresolphthalein (OCP) method, was used to measure the amount of calcium deposited in each group. Alizarin Red S staining was performed on cells grown with SMV loaded membranes to further evaluate their osteogenic potential (Supplementary Information).

2.13. Statistical analysis

All data are presented as mean ± standard deviation, except the molecular modeling data. Significant differences in cytotoxicity of SMV concentration, and *in vitro* bioactivity analyses were analyzed by one-way ANOVA test followed by post-hoc analysis. For the calcium-phosphate mineral deposition assay with membranes, significant difference between

same groups at different time points was analyzed by student t-test. The differences in groups and experimental time points at any time were considered significant if $p < 0.05$

3. RESULTS

3.1. SEM

All membranes exhibited smooth fibers with diameters in the nano-range in scanning electron micrographs (Fig. 1). The as spun membranes (1A) had fibers around 200–300nm, which did not change significantly after the treatments (1B-E). SEM images of SMV loaded membranes also did not show significant changes in the fiber diameter (SI 1).

3.2. ATR-FTIR

ATR spectroscopy was used to analyze the change in the chemical structure of chitosan after the different treatments. Fig. 2 shows the spectra of as spun chitosan membrane and membranes after post-spinning treatments. The broad peak between 3100 and 3500cm^{-1} represents the inter- and intra-molecular hydrogen bonding of the -NH_2 and -OH stretching vibration of chitosan molecules [20]. The absorption peak around 1750cm^{-1} represents the acyl (C=O) group, which confirms the acylation reaction. The peaks between 2750 and 3000cm^{-1} represent asymmetrical and symmetrical bending vibrations of the methylene groups, which increased in intensity with increasing FA chain lengths. The ester C=O stretch around 1700–1750cm^{-1} did not show up in the spectrum of tBOC modified membrane as it selectively reacts with the amine groups of chitosan. The transmittance peaks at 720, 802 and 837cm^{-1} representing TFA salts were not seen in the treated membranes, confirming the removal of TFA salts.

3.3. Water contact angle measurements

The measurements of water contact angles after approximately one minute for differently modified chitosan is represented in Table 1. It was observed that the water droplet from the VCA machine remained stable on the AA and BA membranes for 3–5minutes, whereas for the HA and tBOC membranes, the drop remained stable even after 15 minutes. Among all the treatments, tBOC modified membranes were the most hydrophobic (119.3° ±17.4°). For the FA-treated membranes, as the FA chain length increased, the membranes became more hydrophobic. The AA membranes were least hydrophobic, and the HA were most hydrophobic.

3.4. Elemental analysis

The absence of F in the elemental analysis data indicated there was no residual TFA salts left in the membranes after the post spinning treatments (Table 2). The DM of the FAs or the tBOC groups was calculated based on the C/N ratio from elemental analysis and equation 3. The maximum DM per chitin/chitosan monomer unit for the short chain FAs was 2 since there are two reactive -OH groups on each monomer unit. For the AA and BA modified chitosan, the degree of modification was 1 and for the HA membrane it was between 1 and 2. For the tBOC membrane, the theoretical maximum DM is 0.71 (DDA) as only the chitosan unit has an -NH_2 group to react. The DM of tBOC modified chitosan was calculated to be 0.40.

3.5. *In vitro* SMV release study

Amount of SMV released out of the membranes mainly depended on the type of membrane treatment. Thickness of the membranes did not have significant effect on drug release. Representative cumulative release graphs of thick membranes are shown in Fig. 3 (Percentage drug release from the membranes given in SI 2). For all loadings and thicknesses, AA and tBOC membranes exhibited significantly higher initial burst release levels of SMV than the other two treatments. There was no difference in the release between the BA and HA modified membranes. For all loadings, AA and tBOC membranes released 10–15μg/ml SMV on day 1, whereas the other two membrane groups released less than 5μg/ml. Amount of drug released from the membranes decreased till day 7, after which all the membranes released ~1μg/ml per day. For HA membranes, the initial loading amounts did not seem to influence the release amount, as all the membranes released only around 20μg by the end of 28 days. The BA membranes also had a similar release pattern, however, 500μg SMV loaded BA released more than other BA loaded membranes.

Table 3 summarizes the percentage release from thick membranes after 28 and 91 days of release. At the end of 28 days, AA and tBOC loaded with 500μg SMV released close to 20% of the drug, whereas the corresponding HA and BA membranes released less than 10%. As the loading amount was halved (250μg), the amount released almost doubled for all the membranes. Similar effects were seen when the membranes were loaded with 100 and 50μg SMV. By the end of 91 days, only the AA and tBOC membranes loaded with 50μg SMV released 100% of the drug. The 100μg loaded membranes released close to 50% of the drug, the 250μg close to 40% and the 500μg close to 30%. The BA membranes released almost half the amounts released by the AA and tBOC membranes for the corresponding loading amounts. This was also true for HA100 and HA50 membranes. However, HA500 and HA250 released less than 20% of the drug even after 91 days.

3.6. Determination of solubility and Flory-Huggins parameter ($X_{1,2}$) of SMV with chitosan and differently modified chitosan

The results for the determination of the HSPs for the differently modified chitosans and different forms of SMV are summarized in Table 4. For estimating solubility parameters of chitosan and modified chitosan, we assumed 70% glucosamine and 30% acetylglucosamine and used an average DM = 1 for all the modifications. Results of calculations for Flory-Huggins interaction parameter ($\chi_{1,2}$) between SMV and polymer using the $A_{1,2}$ assumption for the HSP and $\Delta\delta_T^2$ parameter are shown in Table 4 and 5.

The schematics of chemical structures for chitosan and differently modified chitosan is represented in Fig. 4.

It is seen that the solubility and interaction parameters for hydrolyzed SMV is about 2–3 times lower than unhydrolyzed SMV (Table. 5). A lower value indicates better compatibility between the drug and polymer. Results also indicate that as the fatty acid chain length increased, the drug became more compatible to the polymer. The BA and HA modified chitosan had lower $\chi_{1,2}$ values for SMV and hydrolyzed SMV as compared to AA and

tBOC modified chitosan which corresponds to the slower drug release from BA and HA membranes and faster release from the other two.

3.7. Cytotoxicity evaluation of SMV

Results of the 24 and 72 hour cytotoxicity tests of SMV to the W-20-17 cells based on the Cell Titer glo assay was normalized to 0ng/ml SMV. The results indicated that concentrations up to 600ng/ml SMV showed more than 70% cell viability (Fig. 5). This trend was seen at 24 and 72 hours. However, concentrations more than 600ng/ml had toxic effect on the cells. As a result, further experiments were conducted with 600ng/ml SMV as the highest testing concentration.

The results of cell viability and growth over 7 days with AA (0 & 50) and HA (0 & 50) membranes are shown in Fig. 6. Results are reported as percent of cell in control wells that did not contain membranes. Only cells exposed to AA50 membranes showed a statistically significant reduction in cell viability at each time point ($p<0.05$). There were no statistical differences in percent viability and growth of cells between the AA0, HA0 and HA50 membranes ($p>0.05$).

3.8. Cell responses to SMV and SMV loaded membranes

W-20-17 cells were cultured for up to 21 days to evaluate the osteogenic potential of SMV. Cells were evaluated for ALP activity as a marker of osteoblastic differentiation and for calcium-phosphate deposition via OCP reaction, as indicator of terminal differentiation and matrix mineralization. Cells showed a positive dose dependent expression of ALP to increasing concentrations of SMV up to 600ng/ml. (Fig. 7a). Cells grown in the presence of 600ng/ml SMV showed significantly higher ALP activity as compared to the TCP group on days 7 ($p=0.042$), and 21($p=0.021$). On day 14, cells cultured with 600ng/ml SMV exhibited higher ALP activity as compared to TCP control, though the values were not statistically significant at $p=0.05$ ($p=0.08$). By day 21, cells grown with 300ng/ml SMV also exhibited higher ALP activity as compared to TCP group, though not statistically significant ($p=0.18$).

For cells grown in the BMP-2 medium, there was no SMV dose response of ALP activity by the cells, though there was a trend for SMV to enhance the stimulatory effect of BMP-2 on the ALP activity (Fig. 7b). On day 7, only 600ng/ml SMV group showed significantly higher ALP activity than the TCP group ($p=0.025$) but on day 21, all SMV groups showed higher ALP activity than TCP group ($p=0.04$). Overall, the BMP-2 medium groups showed much higher ALP activity as compared to the corresponding regular medium groups. All groups showed increase in ALP activity with culture time.

As a measure of terminal differentiation, amount of calcium deposited by the cells was quantified. When testing different drug concentrations, all the groups showed an increase in the amount of calcium deposited from day 14 to day 21 (Fig. 8). Similar to ALP activity, for the regular medium groups, there was a dose-dependent increase in calcium deposition with increasing SMV concentration. On day 14, 600ng/ml SMV stimulated significantly higher calcium deposition than other groups ($p=0.024$). By day 21, this effect continued ($p= 0.019$). Cells cultured with 300ng/ml SMV also showed a trend to stimulate more calcium deposition, though not significantly higher than control group ($p=0.065$). Among the BMP-2

medium groups also there was a trend for increased calcium deposition with increase in SMV concentration, though none of the groups were significantly different ($p>0.05$). More calcium deposition by the 600ng/ml SMV was evident on day 14 and 21 in both media groups.

Since AA50 membranes showed significant toxicity from day 1, they were not included further for *in vitro* experiments. Fig. 9 shows that the ALP activity of all the groups increased over the period of 21 days. In regular medium group (Fig. 9(a)), on day 7, cells grown with HA50 membranes showed significantly higher ALP activity than the control ($p=0.015$). On day 21, though the SMV loaded membrane, HA50, appeared to stimulate more ALP activity than its corresponding non-loaded membranes, no groups were significantly different from each other and the control ($p=0.81$). In BMP-2 medium group (Fig. 9(b)), on day 14, HA0 group had significantly less ALP activity than the control ($p=0.030$), whereas the loaded membranes and control had similar activities. By day 21, all the membrane groups showed lowered ALP activity than the control ($p=0.034$).

While analyzing the SMV loaded membranes for calcium deposition, in regular medium groups, only the control and HA50 membrane groups showed statistically significant increase in calcium levels from day 14 to 21 (Fig. 10). In BMP-2 medium groups, similar to ALP activity, HA50 group appeared to stimulate more calcium deposition, but none of the groups were significantly different. All groups showed significantly higher calcium deposition on day 21 than day 14. All the BMP-2 medium groups showed significantly higher calcium deposition than regular medium groups. This was also evident with alizarin red S staining of the well plates (SI 3). All the BMP-2 groups stained much darker than the regular medium groups.

4. Discussion

ESCM modified by capping amine groups with tBOC or by grafting short chain FA to the –OH groups on the polymer maintain their nanofiber structure in aqueous environments and exhibit *in vitro* and *in vivo* biocompatibility and degradation properties appropriate for GBR applications [17, 20, 21]. To take advantage of the increased surface area of the nanofibers for local drug delivery, this study showed that membrane modifications can be used to control the release of SMV, an anti-cholesterol drug that also exhibits osteogenic effects and assessed the osteogenic potential of SMV *in vitro* using a mouse stromal cell line.

The tBOC-modified and BA modified ESCM were prepared following previously reported methods [17, 21]. Protocol reported by Wu et al. to FA modify the membranes with BA was modified slightly by using either acetic anhydride or hexanoic anhydride to create the AA- and HA- modified ESCM [20, 21]. FTIR analyses and SEM examinations of membranes demonstrated that all the treatments were effective in removing the TFA salts without causing significant changes to the diameter of the nanofibers of the membranes. Relative changes in the intensity of $-CH_2$ peaks in the FTIR spectra also indicated success in the grafting of AA and HA fatty acids to the chitosan membranes. Similar results were reported by Wu et al. and Su et al., where the treated membranes did not show significant changes in the fiber diameter and the FTIR spectra showed successful grafting of the fatty acid or tBOC

groups[17, 20]. Increase in the water contact angles of the membranes in proportion to the fatty acid chains indicated an increase in the hydrophobic nature of the membranes. In another work by Zhang et al., similar increase in water contact angle with increase in the fatty acid chain length was reported [47]. The longer chain fatty acid had larger water contact angle, suggesting their more hydrophobic nature [47]. Su et al., demonstrated an increase in water contact angle of the tBOC membranes as compared to sodium carbonate treated membranes [17].

Removal of TFA salts and addition of functional groups were further confirmed by elemental analysis, which gave an estimate of DM for each membrane modification. DM for the modified membranes was calculated to be close to 1. However, the values varied slightly based on the treatment. tBOC membranes were determined to have a DM of 0.4, whereas a maximum of 0.71 is possible. This may be due to the inability of the bulky tBOC groups to penetrate the surface of the membrane fibers to react with more chitosan molecules. The shorter AA and BA fatty acid modified membranes had a DM=1, whereas the longer fatty acid modified membranes (HA) on the other hand had a DM of more than 1, which suggests that fatty acid modifications might occur at both -OH groups on the chitosan monomeric units (DM=1 suggests the modification occurs only at one of the -OH groups). The higher DM of HA membranes might also contribute to the more hydrophobic behavior of these membranes. Zhang et al. reported a DM of more than or equal to 2, for all their fatty acid treated membranes, irrespective of the chain length [47]. Elemental analysis did not detect the presence of fluorine, confirming the removal of TFA salts. Thus, all the treatments were successful in removing the TFA salts and maintaining the porous nanofibrous structure of ESCM by increasing their hydrophobic behavior.

As the treatment procedures were able to retain the porous structure of these membranes and modulate their hydrophobic behavior, their ability to deliver a hydrophobic agent was evaluated using a hydrophobic osteogenic drug- SMV. Generally, drug release from polymer-based systems depends on initial drug loading amount, polymer-drug interactions, polymer degradability and the extent of diffusion [48]. The factors analyzed in this study are (1) initial drug loading amount, (2) hydrophobicity of the membranes, (3) thickness of the membranes and (4) polymer-drug interactions. The general concept of like dissolves like was reflected with fatty acid treated membranes. Hydrophobic SMV interacted more with hydrophobic HA and BA membranes, thereby releasing out very slowly. As the hydrophobicity of the membranes decreased, the rate and amount of drug released out of the membranes increased. However, this was not true for the tBOC membranes. Though these membranes were more hydrophobic than HA membranes, based on the water contact angle data, their release was similar to AA membranes. Molecular modeling data using Hansen solubility parameter [45], revealed a high δ_T value for tBOC modified chitosan, which indicated a more hydrophilic character of the polymer as compared to the low δ_T value of the HA and BA modified polymer. As the δ_T value for a compound decreases, it is expected to become more hydrophobic. High water contact angle of tBOC membranes, their high δ_T value and low DM suggest that the tBOC treatment might only be a surface phenomenon. The bulky tBOC groups might have attached only to the $-NH_2$ units present on the surface and might not have been able to penetrate within the fibers to react throughout the membrane's thickness. From the modeling data it was evident that as the fatty acid chain

length increased, the hydrophobic character of the polymer increased. SMV had a low δ_T indicating its hydrophobic character. Since the δ_T values for tBOC and AA membranes were large, they released SMV at a faster rate as compared to the HA and BA membranes that had lower δ_T values.

Further, the large solubility differences ($A_{1,2}$) between SMV (unhydrolyzed) and polymers indicate minimum interaction between the drug and the membranes. Even the most hydrophobic HA membranes seemed to have large $A_{1,2}$ values with the hydrophobic SMV. However, SMV quickly hydrolyzes within few hours in aqueous environment. This hydrolyzed form had smaller $\chi_{1,2}$ values with the modified polymers, indicating enhanced polymer-drug interaction. As the interaction parameter, $\chi_{1,2}$, decreases, the polymer increasingly becomes a better thermodynamic solvent for the drug, resulting in improved drug solubility. As a result, the drug tended to stay within the membranes, rather than diffuse out. These results indicate that our modified chitosan membranes can be used to locally deliver hydrophobic drugs (other than SMV, as well) in a slow and controlled manner.

The exact structures of modified chitosan could not be determined using elemental analysis, since there are two -OH positions available for modification on the acetylated and deacetylated rings of chitosan. We speculate that the fatty acid anhydride would react with primary -OH group faster, with the possibility of reacting with the secondary -OH group. The DM >1 of HA modified chitosan indicated this possibility. Thus, though elemental analysis gave varying DM for each treatment, a DM=1 was assumed for all cases for computational modeling, to purely compare the effect of modified groups on the solubility parameters. Since the most hydrophobic HA had the highest DM, the actual solubility parameter might be even closer to hydrophobic (hydrolyzed) SMV if the DM from elemental analysis was used for the computational analysis, therefore giving the same result. These results confirm our ability to control the release of SMV from chitosan membranes subjected to different modification reactions.

Previous attempts to develop a delivery system for SMV had little success in controlling the drug release as most of the drug released from different scaffolds and vehicles within the first one or two weeks [29, 49, 50]. SMV loaded hydroxyapatite (HAP) microspheres, released 20% of the loaded drug within first 2 hours and reached equilibrium within 3 days after which no significant SMV released out of the membranes[29]. PLGA/HAP microspheres and PLGA membranes loaded with 1mg SMV released maximum amount of the loaded drug within 8 and 4 days, respectively, before reaching equilibrium [50, 51]. In contrast to these studies, 500 and 250μg SMV loaded ESCM treated with AA, BA and tBOC were able to release significant amount of drug even after 91 days of elution without reaching equilibrium, whereas release from only 50μg loaded SMV membranes reached equilibrium close to day 12. Because of strong interaction between HA modified membranes and SMV, these membranes reached equilibrium early (between day 12–14) irrespective of the initial loading amount. These results indicate that our modified membranes can be used to release SMV (and other similar hydrophobic drugs) in different patterns based on the clinical requirement.

Different concentrations of SMV were evaluated in direct contact with mouse bone-marrow stromal cells to check their cytocompatibility and osteogenic potential. Several papers report a maximum of ~400ng/ml (1μM) SMV as the highest drug concentration tolerated by cells like adipose derived stromal cells, mouse bone marrow derived mesenchymal stem cells (MSCs) and human bone marrow stromal cells, to name a few [26, 39, 52]. However, in our work W-20-17 cells showed a slightly higher tolerance to SMV (600ng/ml) as compared to other cell types.

In this study, the osteogenic potential of SMV with and without BMP-2 was evaluated. Additionally, 25ng/ml BMP-2 was added to the cell culture medium to evaluate any adjunctive positive interaction between SMV and BMP-2, since some amount of BMP-2 would be anticipated in the bone healing sites *in vivo*. This level of BMP-2 was selected because 25ng/ml BMP-2 was the least concentration of BMP-2 which induced noticeably higher ALP activity than the control cells. Since BMP-2 was used as the positive control, W-20-17 cells were used for these experiments as they show a dose-dependent increase in ALP with increase in BMP-2 concentration [53–56]. ALP is considered to be an early osteogenic marker, which indicates the beginning of differentiation phase. The dose dependent response of ALP and calcium with increasing levels of SMV, and additional enhanced effect in the presence of BMP-2 is similar to previous studies by Park et al. and Shao et al. [57, 58]. Park et al. reported MC3T3 cells in the presence of 400ng/ml SMV and 60ng/ml BMP-2 showed enhanced osteogenic differentiation, as compared to 400ng/ml SMV alone [57], which was similar to the effect shown by the W-20-17 cells. SMV is known to antagonize TNF-α inhibition of BMPs [30]. Since the W-20-17 cells produce ALP in response to BMP-2 in a dose dependent manner, prolonged presence of BMP-2 (due to SMV's action on TNF-α) in addition to the BMP-2 added to the culture medium might have induced higher ALP activity by the cells, leading to better mineralization. In addition to antagonizing TNF-α, SMV may augment BMP-2 effects by stimulating the expression of α5-integrin and smad molecules, both of which play critical roles in stimulating osteogenesis [57, 58]. SMV is thought to bind to the integrin molecules and induce phosphorylation of FAK, which in turn mediates the BMP-2/smad pathway [59, 60]. In MC3T3 cells, FAK phosphorylation induces the activation of Runx2, which is a key regulator of osteoblast differentiation and also is important in the expression of ALP and OCN in the differentiation process [61]. The smad molecule is known to mediate the canonical signaling cascade of TGF-β superfamily growth factors, of which BMPs are a member [62]. Taken together these data strongly suggest that SMV does have a positive interaction with BMP-2 at stimulating bone differentiation and may be beneficial for bone healing and regeneration.

Since the adequate dosage and extent of drug release that would stimulate sufficient osteogenesis is not known, membranes with different release profiles were evaluated in this study. To avoid any cytotoxicity issues due to high drug concentrations, only low drug dose membranes were considered. The membranes tested in this work were selected to provide either fast release of low dose (AA50) or slow release of a low dose (HA50). In this study, with the exception of AA50 membranes, the non-loaded HA and AA and HA50 membranes showed a cell viability of more than 70%, indicating non-toxicity of our membranes. The amount of drug released out of the AA50 membranes on day 1, around 10–12μg, may have

been toxic to the cells. Another study where SMV- loaded chitosan nanoparticles were investigated, similar and higher amounts of SMV released from the particles did not show any toxicity to the bone marrow stromal cells tested [49]. However, the same range of SMV was toxic to rat bone MSCs when delivered from HAP microspheres [29].

While evaluating the osteogenic potential of SMV-loaded membranes, for regular medium groups, ALP activity increased over time. HA50 membranes showed a trend for increased ALP activity over non-loaded membrane groups, starting on day 7, indicating the osteogenic potential of SMV, similar to the results obtained when SMV was directly added to the cells dispersed in cell culture medium. When membranes were combined with medium containing BMP-2 to explore any adjunctive effects, the results showed that there was a trend of higher ALP activity in the presence of HA50 membranes as compared to HA0, again similar to when SMV and BMP-2 were added directly to the cells together. Interestingly in the BMP-2 medium groups, all the membrane groups showed lower ALP activity than the control. This was thought to be because of chitosan's ability to chelate BMP-2, thereby lowering its activity [63].

In case of calcium-phosphate deposition as measured by the OCP assay, the HA50 membranes showed higher mineralization as compared to HA0 membranes (with no significant difference between control and HA50 membranes) in regular and BMP-2 supplemented media groups. Overall, cells grown with BMP-2 supplemented medium showed higher mineralization than those grown in regular medium. Yu et al. reported an increased ALP and OCN expression in rat bone marrow MSCs by day 7 when they were incubated with SMV-loaded HAP microspheres (as compared to non-loaded spheres groups and cells alone control). The amount of SMV released from these particles was 1–2μg/ml till day 3, [29] which was similar to the amount of SMV released from the HA50 membranes. In another study, Xue et al. reported SMV loaded chitosan nanoparticles to stimulate significantly higher ALP activity in bone marrow stromal cells, than non-loaded particles only by day 14, since the daily release of SMV was close to only 0.2μg/ml [49]. However, such low levels of SMV released from HAP-PLGA particles triggered a higher ALP activity, OCN expression and calcium deposition in mouse MSCs within 3 days of culture [50]. Nonetheless, the results from our experiments suggest that the ESCMs are able to release SMV in a slow and sustained manner and the released SMV has a positive effect on osteogenesis on its own and in conjunction with BMP-2, thereby highlighting our membranes' potential to locally deliver drugs to the defect site.

Because of the wide range of effective SMV dose *in vitro*, the ideal release profile of the drug is still not clear. It is speculated that a sustained release may be appropriate. The inability of HA50 membranes to stimulate significantly higher mineralization than the controls could be due to the strong interaction between hydrophobic HA modified chitosan and hydrophobic SMV, which might have prevented higher amounts of SMV from releasing out of the membranes. However, the long sustained release may be advantageous in a clinical setting, where the bone healing process will start only after 2–3 weeks of injury. Thus, having a drug delivery system which can retain and release the drug for prolonged time frames might be useful in promoting better bone regeneration. The modifications used in this work provide a means for investigating these types of SMV release profiles from

ESCM for determining effective dosing strategies for stimulating bone regeneration. Further, evaluating these SMV-loaded membranes with other commonly used bone cell types, like MC3T3 or Saos-2, might provide a better insight into their osteogenic potential.

5. Conclusion

Release of SMV from ESCM was controlled by subjecting the membranes to different fatty acid or amine-capping treatments and by loading different initial drug amounts. Since these membranes have already shown to support and guide bone regeneration, our ability to control the release of a potential osteogenic drug from these membranes would enable us to customize the membranes based on the clinical need. *In vitro* release and cell culture studies with SMV-loaded membranes highlight the unique ability of our membranes to locally deliver hydrophobic drugs in a sustained manner for up to 90 days that has not been achieved by other methods and that the released SMV positively impacts osteogenic differentiation of the W-20-17 bone cells alone and in presence of BMP-2. Next, these drug-loaded membranes need to be evaluated with other bone cell types and in an *in vivo* model, to better understand their osteogenic potential. Further, these membranes can also be used as a platform to deliver hydrophobic drugs, such as cancer therapeutics, that are difficult to deliver locally in a sustained manner.

Supplementary Material

Refer to Web version on PubMed Central for supplementary material.

Acknowledgement

This study was funded by a grant from the National Institute of Health- National Institute of Dental & Craniofacial Research (R01DE026759) and was also supported by the Biomaterials Applications of Memphis (BAM) laboratories in the Biomedical Engineering Department at The University of Memphis. Dr. Fernanda Delbuque Guerra and Dr. Kwei-Yu Liu helped with the HPLC and FTIR training.

References

[1]. Xu C, Lei C, Meng L, Wang C, Song Y, Chitosan as a barrier membrane material in periodontal tissue regeneration, Journal of Biomedical Materials Research Part B: Applied Biomaterials, 100 (2012) 1435–1443.

[2]. Norowski PA Jr, Fujiwara T, Clem WC, Adatrow PC, Eckstein EC, Haggard WO, Bumgardner JD, Novel naturally crosslinked electrospun nanofibrous chitosan mats for guided bone regeneration membranes: Material characterization and cytocompatibility, Journal of tissue engineering and regenerative medicine, 9 (2015) 577–583. [PubMed: 23166109]

[3]. Park H, Choi B, Hu J, Lee M, Injectable chitosan hyaluronic acid hydrogels for cartilage tissue engineering, Acta biomaterialia, 9 (2013) 4779–4786. [PubMed: 22935326]

[4]. Wang JJ, Zeng ZW, Xiao RZ, Xie T, Zhou GL, Zhan XR, Wang SL, Recent advances of chitosan nanoparticles as drug carriers, International journal of nanomedicine, 6 (2011) 765. [PubMed: 21589644]

[5]. Chen Z, Wang P, Wei B, Mo X, Cui F, Electrospun collagen–chitosan nanofiber: A biomimetic extracellular matrix for endothelial cell and smooth muscle cell, Acta Biomaterialia, 6 (2010) 372–382. [PubMed: 19632361]

[6]. Bhattarai N, Edmondson D, Veiseh O, Matsen FA, Zhang M, Electrospun chitosan-based nanofibers and their cellular compatibility, Biomaterials, 26 (2005) 6176–6184. [PubMed: 15885770]

[7]. Jayakumar R, Prabaharan M, Nair S, Tamura H, Novel chitin and chitosan nanofibers in biomedical applications, Biotechnology advances, 28 (2010) 142–150. [PubMed: 19913083]

[8]. Noel SP, Courtney H, Bumgardner JD, Haggard WO, Chitosan films: a potential local drug delivery system for antibiotics, Clinical orthopaedics and related research, 466 (2008) 1377–1382. [PubMed: 18421540]

[9]. Mendes AC, Gorzelanny C, Halter N, Schneider SW, Chronakis IS, Hybrid electrospun chitosan-phospholipids nanofibers for transdermal drug delivery, International journal of pharmaceutics, 510 (2016) 48–56. [PubMed: 27286632]

[10]. Ali A, Ahmed S, A review on chitosan and its nanocomposites in drug delivery, International journal of biological macromolecules, 109 (2018) 273–286. [PubMed: 29248555]

[11]. Norowski PA, Babu J, Adatrow PC, Garcia-Godoy F, Haggard WO, Bumgardner JD, Antimicrobial Activity of Minocycline-Loaded Genipin-Crosslinked Nano-Fibrous Chitosan Mats for Guided Tissue Regeneration, Journal of Biomaterials and Nanobiotechnology, 3 (2012) 528.

[12]. Lee E-J, Kim H-E, Accelerated bony defect healing by chitosan/silica hybrid membrane with localized bone morphogenetic protein-2 delivery, Materials Science and Engineering: C, 59 (2016) 339–345.

[13]. Shin SY, Park HN, Kim KH, Lee MH, Choi YS, Park YJ, Lee YM, Ku Y, Rhyu IC, Han SB, Biological evaluation of chitosan nanofiber membrane for guided bone regeneration, Journal of periodontology, 76 (2005) 1778–1784. [PubMed: 16253101]

[14]. Yeo YJ, Jeon DW, Kim CS, Choi SH, Cho KS, Lee YK, Kim CK, Effects of chitosan nonwoven membrane on periodontal healing of surgically created one-wall intrabony defects in beagle dogs, Journal of Biomedical Materials Research Part B: Applied Biomaterials: An Official Journal of The Society for Biomaterials, The Japanese Society for Biomaterials, and The Australian Society for Biomaterials and the Korean Society for Biomaterials, 72 (2005) 86–93.

[15]. Chesnutt BM, Yuan Y, Buddington K, Haggard WO, Bumgardner JD, Composite chitosan/nano-hydroxyapatite scaffolds induce osteocalcin production by osteoblasts in vitro and support bone formation in vivo, Tissue Engineering Part A, 15 (2009) 2571–2579. [PubMed: 19309240]

[16]. Kuo SM, Chang SJ, Chen TW, Kuan TC, Guided tissue regeneration for using a chitosan membrane: an experimental study in rats, Journal of Biomedical Materials Research Part A: An Official Journal of The Society for Biomaterials, The Japanese Society for Biomaterials, and The Australian Society for Biomaterials and the Korean Society for Biomaterials, 76 (2006) 408–415.

[17]. Su H, Liu K-Y, Karydis A, Abebe DG, Wu C, Anderson KM, Ghadri N, Adatrow P, Fujiwara T, Bumgardner JD, In vitro and in vivo evaluations of a novel post-electrospinning treatment to improve the fibrous structure of chitosan membranes for guided bone regeneration, Biomedical materials (Bristol, England), 12 (2016) 015003–015003.

[18]. Ohkawa K, Cha D, Kim H, Nishida A, Yamamoto H, Electrospinning of chitosan, Macromolecular rapid communications, 25 (2004) 1600–1605.

[19]. EL-HAFIAN EA, Elgannoudi ES, Mainal A, Yahaya AHB, Characterization of chitosan in acetic acid: Rheological and thermal studies, Turkish Journal of Chemistry, 34 (2010) 47–56.

[20]. Wu C, Su H, Tang S, Bumgardner JD, The stabilization of electrospun chitosan nanofibers by reversible acylation, Cellulose, 21 (2014) 2549–2556.

[21]. Wu C, Su H, Karydis A, Anderson KM, Ghadri N, Tang S, Wang Y, Bumgardner JD, Mechanically stable surface-hydrophobilized chitosan nanofibrous barrier membranes for guided bone regeneration, Biomedical Materials, 13 (2017) 015004.

[22]. Choi SH, Kim CK, Cho KS, Huh JS, Sorensen RG, Wozney JM, Wikesjö UM, Effect of recombinant human bone morphogenetic protein-2/absorbable collagen sponge (rhBMP-2/ACS) on healing in 3-wall intrabony defects in dogs, Journal of periodontology, 73 (2002) 63–72. [PubMed: 11852905]

[23]. Seeherman H, Wozney J, Li R, Bone morphogenetic protein delivery systems, Spine, 27 (2002) S16–S23. [PubMed: 12205414]

[24]. Nyan M, Hao J, Miyahara T, Noritake K, Rodriguez R, Kasugai S, Accelerated and enhanced bone formation on novel simvastatin-loaded porous titanium oxide surfaces, Clinical implant dentistry and related research, 16 (2014) 675–683. [PubMed: 23399109]

[25]. Priyanka N, Abhilash A, Saquib S, Malgaonkar N, Kudyar N, Gupta A, Kalra N, Pradeep A, Clinical Eficacy of Subgingivally Delivered 1.2 mg Simvastatin in the Treatment of Patients with Aggressive Periodontitis: A Randomized Controlled Clinical Trial, International Journal of Periodontics & Restorative Dentistry, 37 (2017).

[26]. Baek KH, Lee WY, Oh KW, Tae HJ, Lee JM, Lee EJ, Han JH, Kang MI, Cha BY, Lee KW, The effect of simvastatin on the proliferation and differentiation of human bone marrow stromal cells, Journal of Korean medical science, 20 (2005) 438–444. [PubMed: 15953866]

[27]. Thylin MR, McConnell JC, Schmid MJ, Reckling RR, Ojha J, Bhattacharyya I, Marx DB, Reinhardt RA, Effects of simvastatin gels on murine calvarial bone, Journal of periodontology, 73 (2002) 1141–1148. [PubMed: 12416771]

[28]. Nyan M, Sato D, Kihara H, Machida T, Ohya K, Kasugai S, Effects of the combination with α-tricalcium phosphate and simvastatin on bone regeneration, Clinical Oral Implants Research, 20 (2009) 280–287. [PubMed: 19397639]

[29]. Yu W-L, Sun T-W, Qi C, Zhao H-K, Ding Z-Y, Zhang Z-W, Sun B-B, Shen J, Chen F, Zhu Y-J, Enhanced osteogenesis and angiogenesis by mesoporous hydroxyapatite microspheres-derived simvastatin sustained release system for superior bone regeneration, Scientific reports, 7 (2017) 44129.

[30]. Yamashita M, Otsuka F, Mukai T, Otani H, Inagaki K, Miyoshi T, Goto J, Yamamura M, Makino H, Simvastatin antagonizes tumor necrosis factor-α inhibition of bone morphogenetic proteins-2-induced osteoblast differentiation by regulating Smad signaling and Ras/Rho-mitogen-activated protein kinase pathway, Journal of Endocrinology, 196 (2008) 601–613. [PubMed: 18310456]

[31]. Sakoda K, Yamamoto M, Negishi Y, Liao J, Node K, Izumi Y, Simvastatin decreases IL-6 and IL-8 production in epithelial cells, Journal of dental research, 85 (2006) 520–523. [PubMed: 16723648]

[32]. Takenaka M, Hirade K, Tanabe K, Akamatsu S, Dohi S, Matsuno H, Kozawa O, Simvastatin stimulates VEGF release via p44/p42 MAP kinase in vascular smooth muscle cells, Biochemical and biophysical research communications, 301 (2003) 198–203. [PubMed: 12535662]

[33]. Mundy G, Garrett R, Harris S, Chan J, Chen D, Rossini G, Boyce B, Zhao M, Gutierrez G.l., Stimulation of bone formation in vitro and in rodents by statins, Science, 286 (1999) 1946–1949. [PubMed: 10583956]

[34]. Wang PS, Solomon DH, Mogun H, Avorn J, HMG-CoA reductase inhibitors and the risk of hip fractures in elderly patients, Jama, 283 (2000) 3211–3216. [PubMed: 10866868]

[35]. Funkhouser HL, Adera T, Adler RA, Effect of HMG-CoA reductase inhibitors (statins) on bone mineral density, Journal of Clinical Densitometry, 5 (2002) 151–158. [PubMed: 12110758]

[36]. Song C, Guo Z, Ma Q, Chen Z, Liu Z, Jia H, Dang G, Simvastatin induces osteoblastic differentiation and inhibits adipocytic differentiation in mouse bone marrow stromal cells, Biochemical and biophysical research communications, 308 (2003) 458–462. [PubMed: 12914771]

[37]. Qi Y, Zhao T, Yan W, Xu K, Shi Z, Wang J, Mesenchymal stem cell sheet transplantation combined with locally released simvastatin enhances bone formation in a rat tibia osteotomy model, Cytotherapy, 15 (2013) 44–56. [PubMed: 23260085]

[38]. Huang X, Huang Z, Li W, Highly efficient release of simvastatin from simvastatin-loaded calcium sulphate scaffolds enhances segmental bone regeneration in rabbits, Molecular medicine reports, 9 (2014) 2152–2158. [PubMed: 24691672]

[39]. Zhou Y, Ni Y, Liu Y, Zeng B, Xu Y, Ge W, The role of simvastatin in the osteogenesis of injectable tissue-engineered bone based on human adipose-derived stromal cells and platelet-rich plasma, Biomaterials, 31 (2010) 5325–5335. [PubMed: 20381859]

[40]. Jerwood S, Cohen J, Unexpected antimicrobial effect of statins, Journal of antimicrobial chemotherapy, 61 (2007) 362–364. [PubMed: 18086693]

[41]. Ghadri N, Anderson KM, Adatrow P, Stein SH, Su H, Garcia-Godoy F, Karydis A, Bumgardner JD, Evaluation of bone regeneration of simvastatin loaded chitosan nanofiber membranes in rodent calvarial defects, Journal of Biomaterials and Nanobiotechnology, 9 (2018) 210.

[42]. Wong R, Rabie A, Statin collagen grafts used to repair defects in the parietal bone of rabbits, British Journal of Oral and Maxillofacial Surgery, 41 (2003) 244–248. [PubMed: 12946667]

[43]. Tanigo T, Takaoka R, Tabata Y, Sustained release of water-insoluble simvastatin from biodegradable hydrogel augments bone regeneration, Journal of Controlled Release, 143 (2010) 201–206. [PubMed: 20060429]

[44]. Asafo-Adjei TA, Dziubla TD, Puleo DA, Tuning properties of poly (ethylene glycol)-block-poly (simvastatin) copolymers synthesized via triazabicyclodecene, Reactive and Functional Polymers, 119 (2017) 37–46. [PubMed: 29217967]

[45]. Hansen CM, Hansen solubility parameters: a user's handbook, CRC press, 2002.

[46]. Dinescu S, Ionita M, Pandele AM, Galateanu B, Iovu H, Ardelean A, Costache M, Hermenean A, In vitro cytocompatibility evaluation of chitosan/graphene oxide 3D scaffold composites designed for bone tissue engineering, Bio-medical materials and engineering, 24 (2014) 2249–2256. [PubMed: 25226924]

[47]. Zhang Z, Jin F, Wu Z, Jin J, Li F, Wang Y, Wang Z, Tang S, Wu C, Wang Y, O-acylation of chitosan nanofibers by short-chain and long-chain fatty acids, Carbohydrate polymers, 177 (2017) 203–209. [PubMed: 28962759]

[48]. Gunatillake PA, Adhikari R, Biodegradable synthetic polymers for tissue engineering, Eur Cell Mater, 5 (2003) 1–16. [PubMed: 14562275]

[49]. Xue Y, Wu M, Liu Z, Song J, Luo S, Li H, Li Y, Jin L, Guan B, Lin M, In vitro and in vivo evaluation of chitosan scaffolds combined with simvastatin-loaded nanoparticles for guided bone regeneration, Journal of Materials Science: Materials in Medicine, 30 (2019) 47. [PubMed: 30980130]

[50]. Tai I.-c., Fu Y-C, Wang C-K, Chang J-K, Ho M-L, Local delivery of controlled-release simvastatin/PLGA/HAp microspheres enhances bone repair, International journal of nanomedicine, 8 (2013) 3895. [PubMed: 24143094]

[51]. Rashidi H, Ellis MJ, Cartmell SH, Chaudhuri JB, Simvastatin release from poly (lactide- co-glycolide) membrane scaffolds, Polymers, 2 (2010) 709–718.

[52]. Liu Y-S, Ou M-E, Liu H, Gu M, Lv L-W, Fan C, Chen T, Zhao X-H, Jin C-Y, Zhang X, The effect of simvastatin on chemotactic capability of SDF-1α and the promotion of bone regeneration, Biomaterials, 35 (2014) 4489–4498. [PubMed: 24589359]

[53]. Thies RS, Bauduy M, Ashton BA, Kurtzberg L, Wozney JM, Rosen V, Recombinant human bone morphogenetic protein-2 induces osteoblastic differentiation in W-20-17 stromal cells, Endocrinology, 130 (1992) 1318–1324. [PubMed: 1311236]

[54]. Kim S, Tsao H, Kang Y, Young DA, Sen M, Wenke JC, Yang Y, In vitro evaluation of an injectable chitosan gel for sustained local delivery of BMP-2 for osteoblastic differentiation, Journal of Biomedical Materials Research Part B: Applied Biomaterials, 99 (2011) 380–390.

[55]. Balk M, Bray J, Day C, Epperly M, Greenberger J, Evans CH, Niyibizi C, Effect of rhBMP-2 on the osteogenic potential of bone marrow stromal cells from an osteogenesis imperfecta mouse (oim), Bone, 21 (1997) 7–15. [PubMed: 9213002]

[56]. Osyczka AM, Diefenderfer DL, Bhargave G, Leboy PS, Different effects of BMP-2 on marrow stromal cells from human and rat bone, Cells tissues organs, 176 (2004) 109–119. [PubMed: 14745240]

[57]. Park J-B, Combination of simvastatin and bone morphogenetic protein-2 enhances the differentiation of osteoblasts by regulating the expression of phospho-Smad1/5/8, Experimental and therapeutic medicine, 4 (2012) 303–306. [PubMed: 22970034]

[58]. Shao P-L, Wu S-C, Lin Z-Y, Ho M-L, Chen C-H, Wang C-Z, Alpha-5 Integrin Mediates Simvastatin-Induced Osteogenesis of Bone Marrow Mesenchymal Stem Cells, International journal of molecular sciences, 20 (2019) 506.

[59]. Ma X-Y, Feng Y-F, Wang T-S, Lei W, Li X, Zhou D-P, Wen X-X, Yu H-L, Xiang L-B, Wang L, Involvement of FAK-mediated BMP-2/Smad pathway in mediating osteoblast adhesion and differentiation on nano-HA/chitosan composite coated titanium implant under diabetic conditions, Biomaterials science, 6 (2018) 225–238.

[60]. Tamura Y, Takeuchi Y, Suzawa M, Fukumoto S, Kato M, Miyazono K, Fujita T, Focal adhesion kinase activity is required for bone morphogenetic protein—Smad1 signaling and osteoblastic differentiation in murine MC3T3-E1 cells, Journal of bone and mineral research, 16 (2001) 1772–1779. [PubMed: 11585340]

[61]. Ge C, Yang Q, Zhao G, Yu H, Kirkwood KL, Franceschi RT, Interactions between extracellular signal-regulated kinase 1/2 and P38 Map kinase pathways in the control of RUNX2 phosphorylation and transcriptional activity, Journal of Bone and Mineral Research, 27 (2012) 538–551. [PubMed: 22072425]

[62]. Song B, Estrada KD, Lyons KM, Smad signaling in skeletal development and regeneration, Cytokine & growth factor reviews, 20 (2009) 379–388. [PubMed: 19926329]

[63]. Park YJ, Kim KH, Lee JY, Ku Y, Lee SJ, Min BM, Chung CP, Immobilization of bone morphogenetic protein-2 on a nanofibrous chitosan membrane for enhanced guided bone regeneration, Biotechnology and applied biochemistry, 43 (2006) 17–24. [PubMed: 15910285]

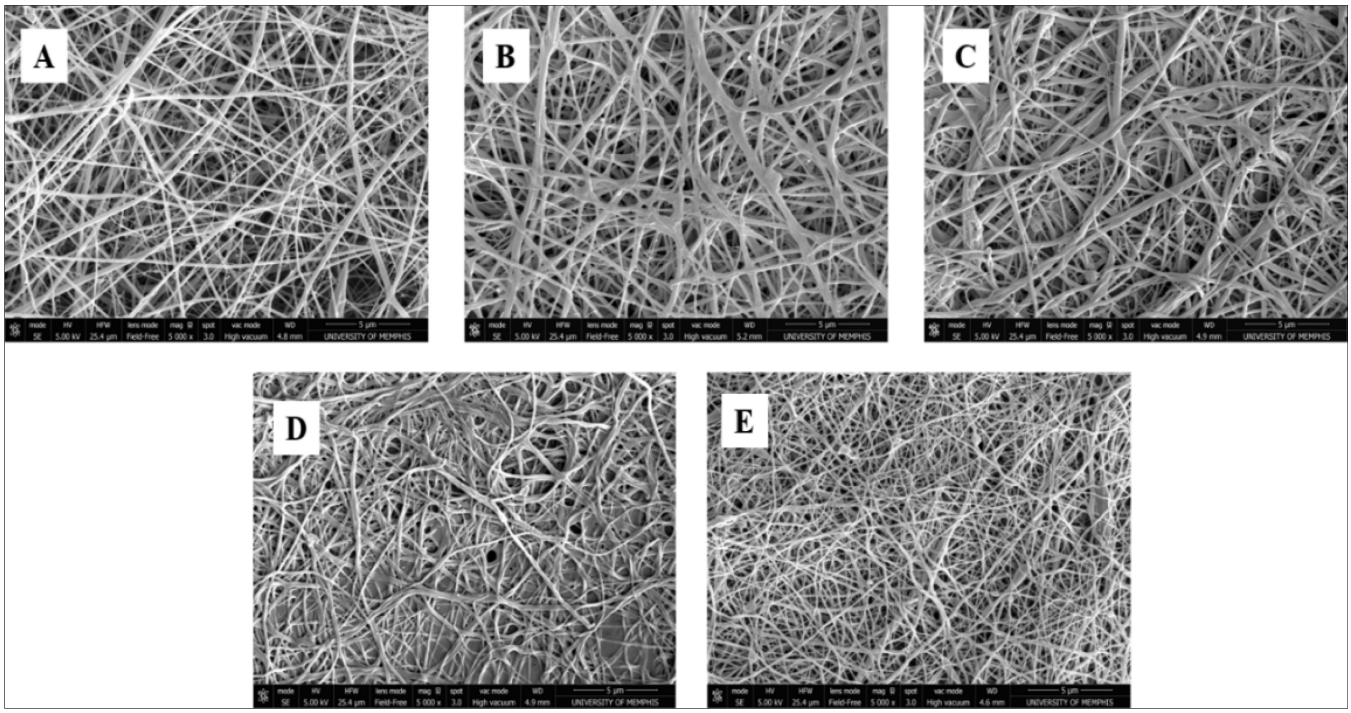

Fig. 1.

Images show micrographs of (A) as spun membrane (B) AA-treated membrane (C) BA-treated membrane (D) HA-treated membrane and (E) TEA-tBOC-treated membrane.

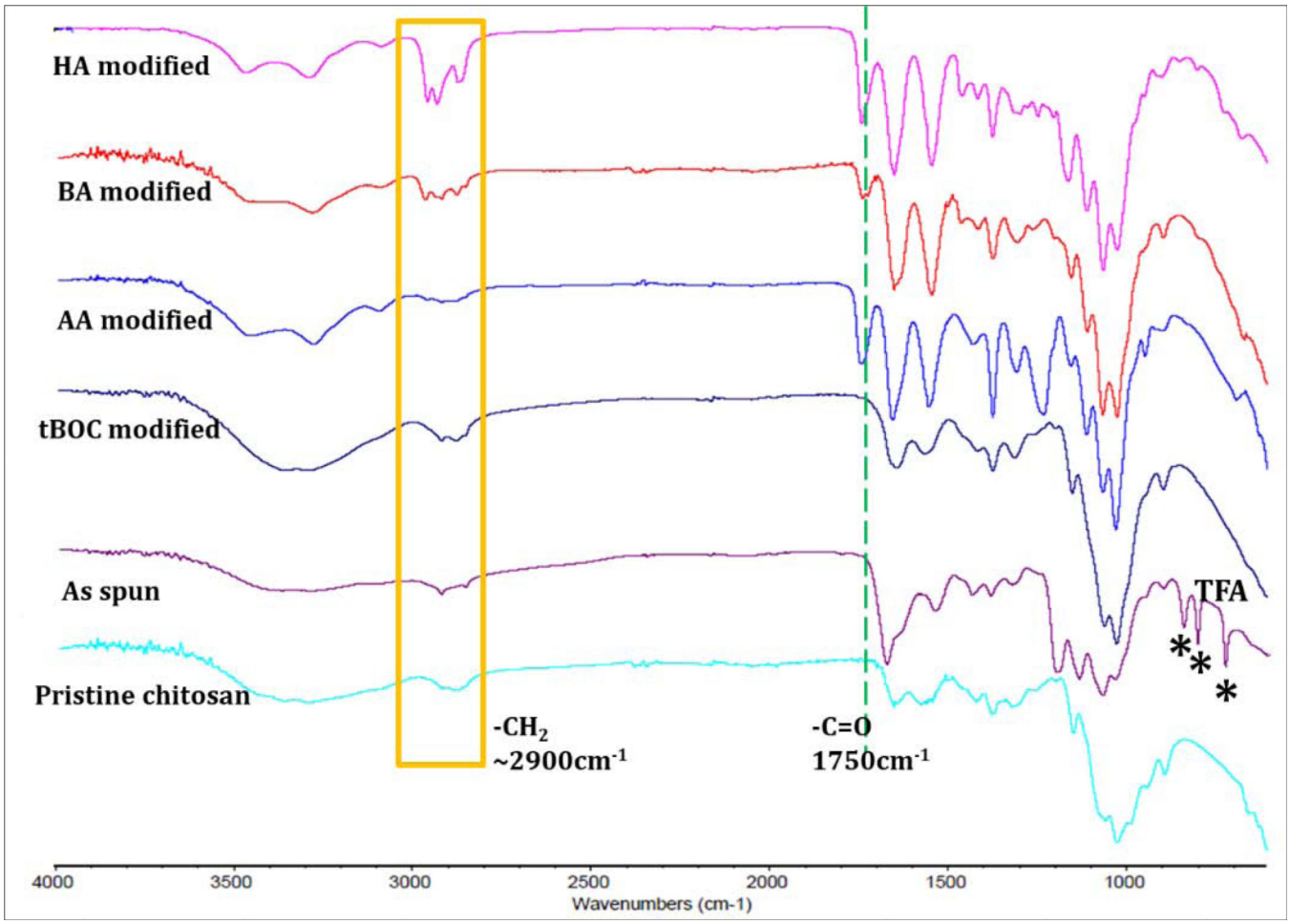

Fig. 2.

ATR spectra of chitosan powder, as spun chitosan, showing the TFA peaks and modified chitosan showing the disappearance of TFA peaks and addition of methyl groups.

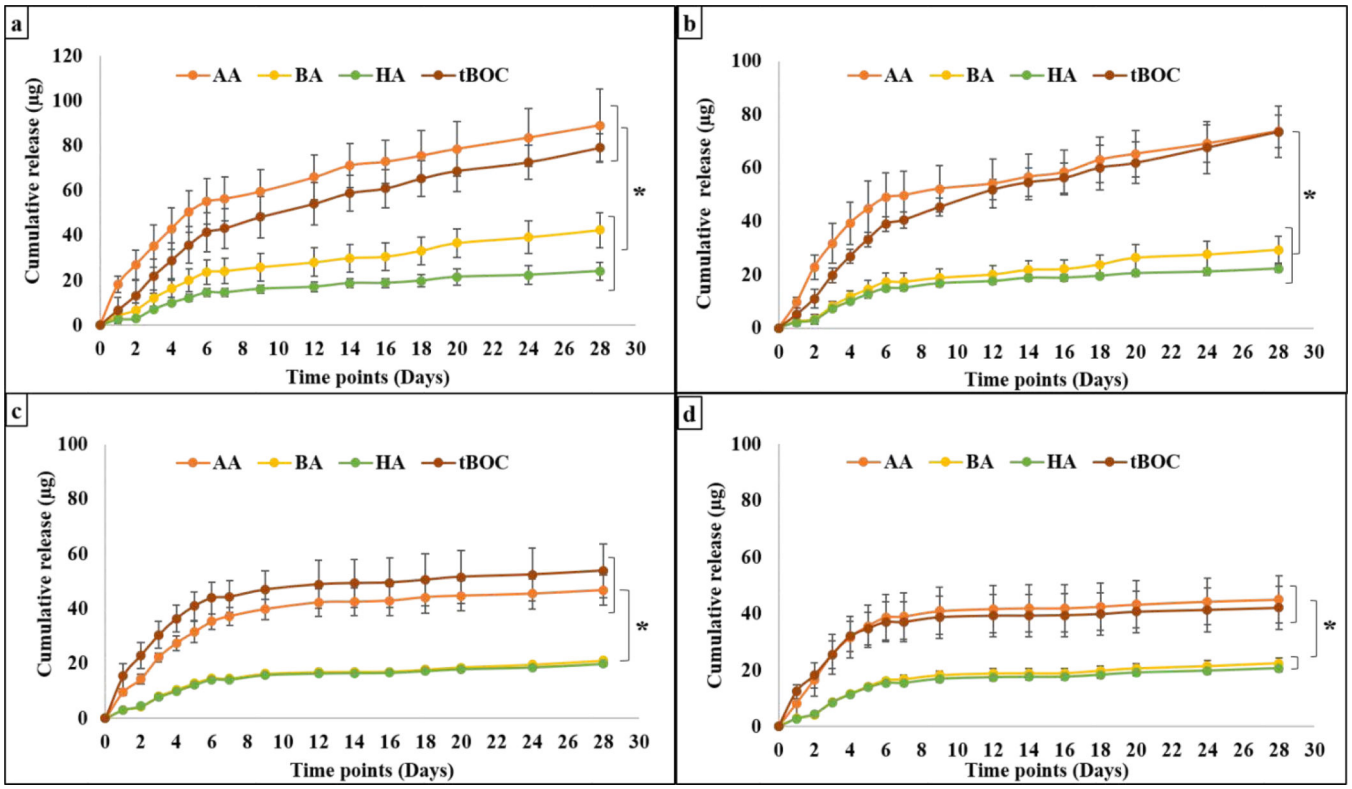

Fig. 3.

Graphs show cumulative release over time for thick membranes treated with either fatty acids or tBOC and loaded with (a) 500µg, (b) 250µg, (c) 100µg and (d) 50µg. The AA and tBOC membranes released higher amounts of drug than BA and HA treated membranes. Each value represents the mean ± SD (n=6). * indicates statistically significant difference with $p < 0.05$.

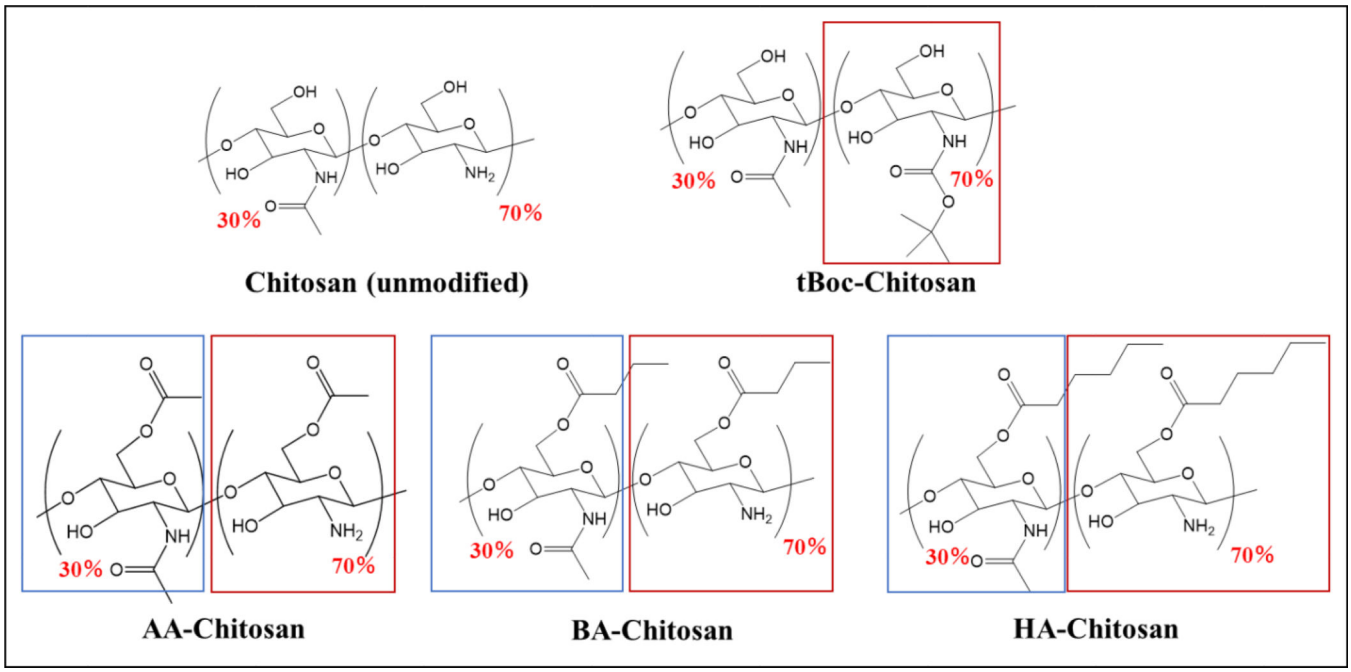

Fig. 4.

Schematic of unmodified and modified chitosan after tBOC and fatty acid treatments. The degree of modification was assumed to be 1 for all the modifications. The tBOC groups attached to amine group of the polymer and the fatty acids reacted with hydroxyl group.

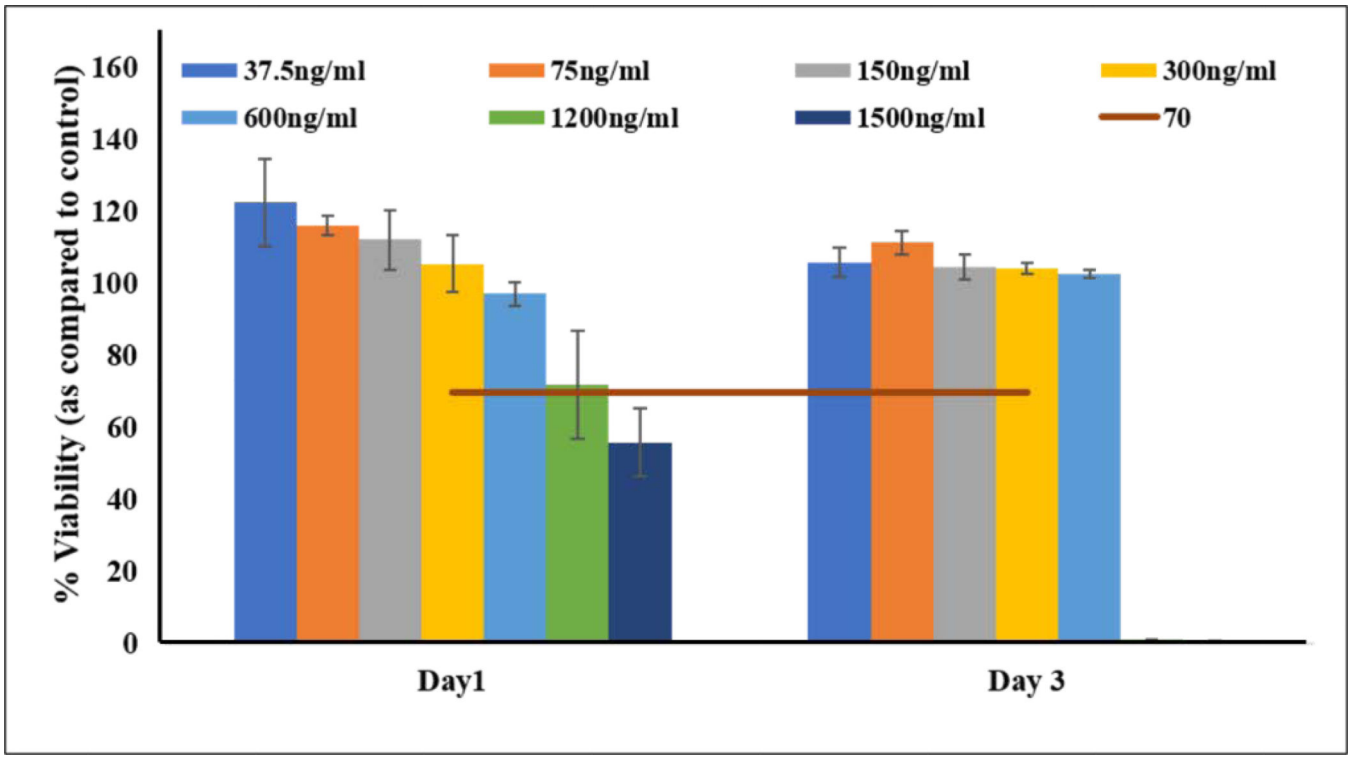

Fig. 5.

Graph shows cell viability expressed as a percentage of control (0ng/ml SMV in medium) for increasing doses of SMV. Each value represents the mean ± SD (n=4). The horizontal line represents 70% cell viability, which is the minimum viability required to be supported by a device to be cytocompatible, according to ISO standard [46].

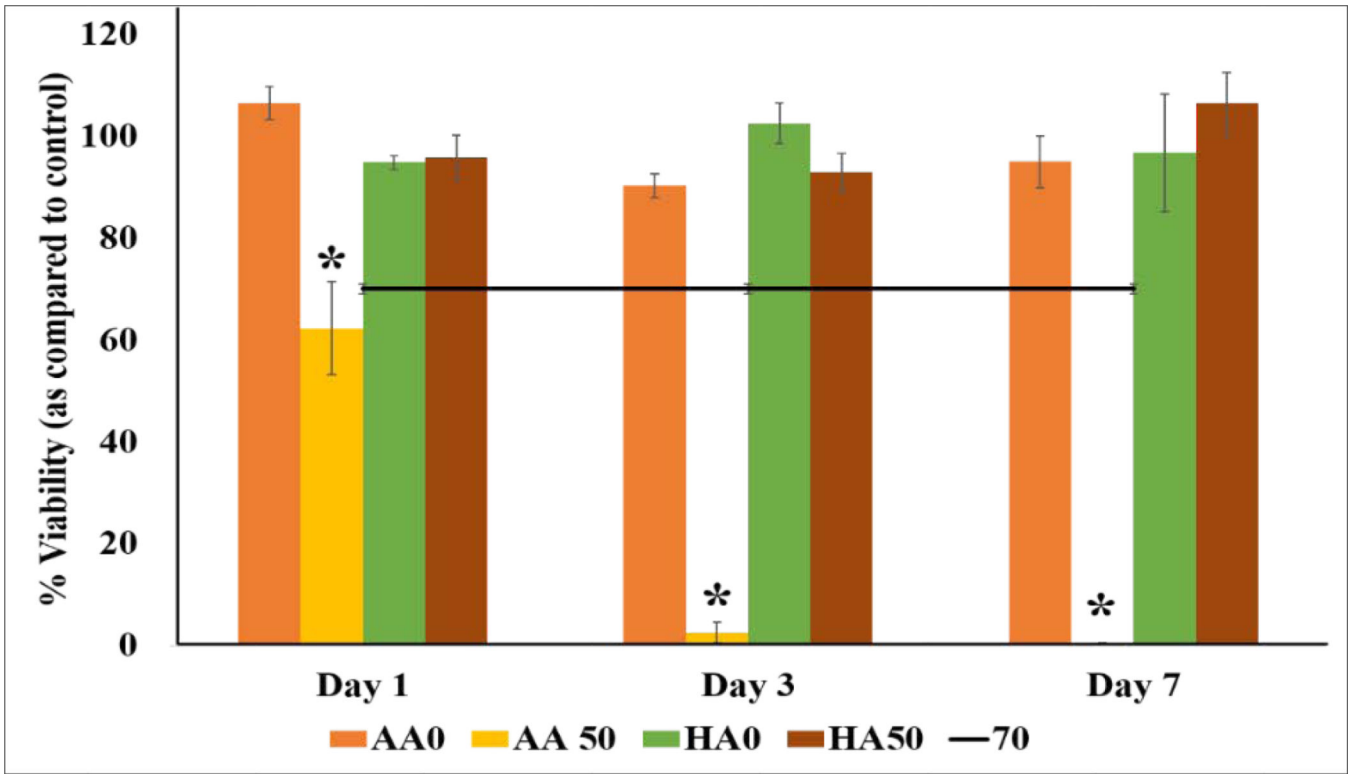

Fig. 6.

Cell viability of W-20-17 cells grown in the presence of different membranes and expressed as % viability as compared to cells grown on tissue culture plastic. Each value represents the mean ± SD (n= 4 per each group). * denotes significant difference among groups at a given time point ($p<0.05$). The bar indicates 70% viability level.

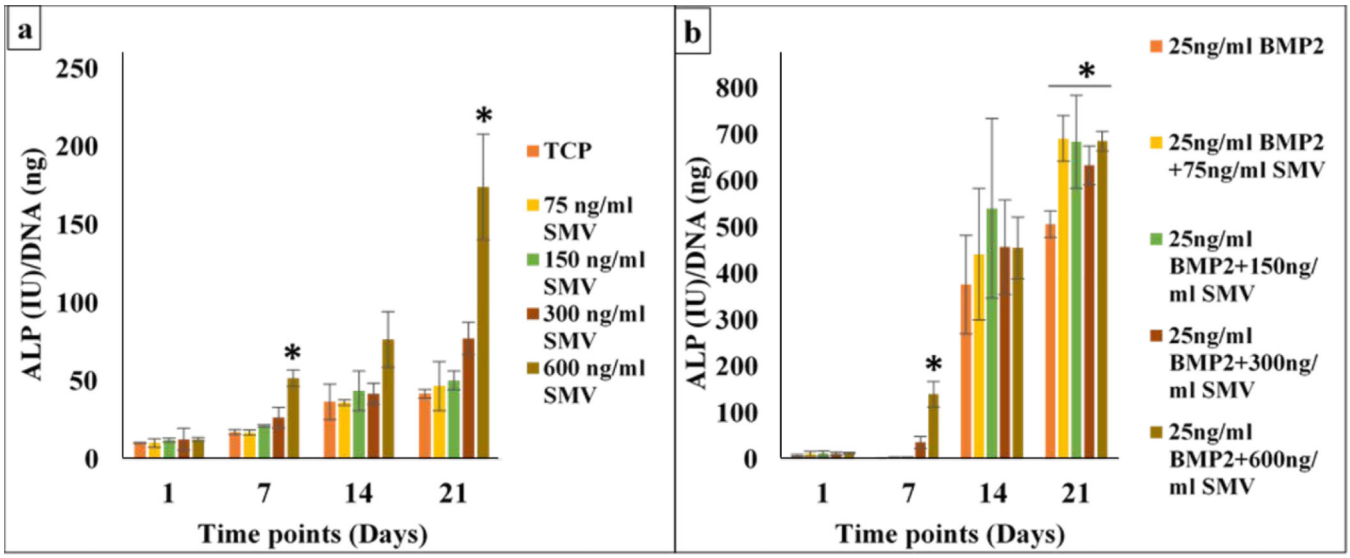

Fig. 7.

The effect of SMV on induction of alkaline phosphatase (ALP) activity in W-20-17 cells in regular media (a) and BMP-2 media (b). Each value represents the mean ± SD (n=4). * indicates significant difference between the experimental group and the TCP (tissue culture plastic) group for that time point ($p<0.05$)

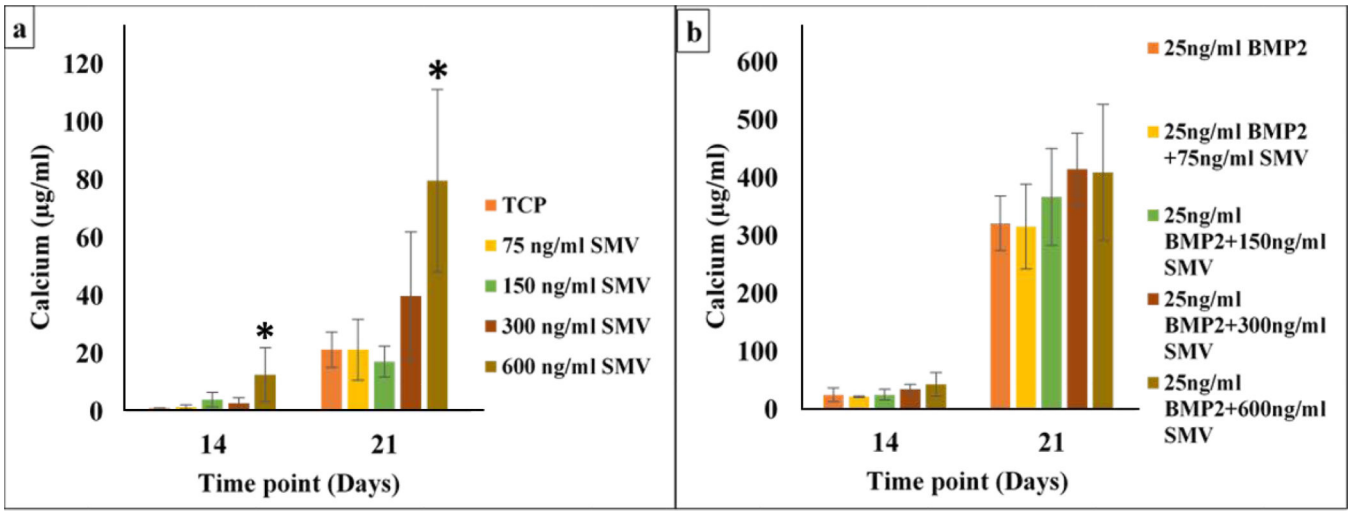

Fig. 8.

Calcium assay to determine the amount of calcium deposited by the cells in the presence of different concentrations of SMV in regular media (a) and BMP-2 media (b). Each value represents the mean ± SD (n=4). * indicates significant difference between the experimental group and the control group for that time point ($p<0.05$)

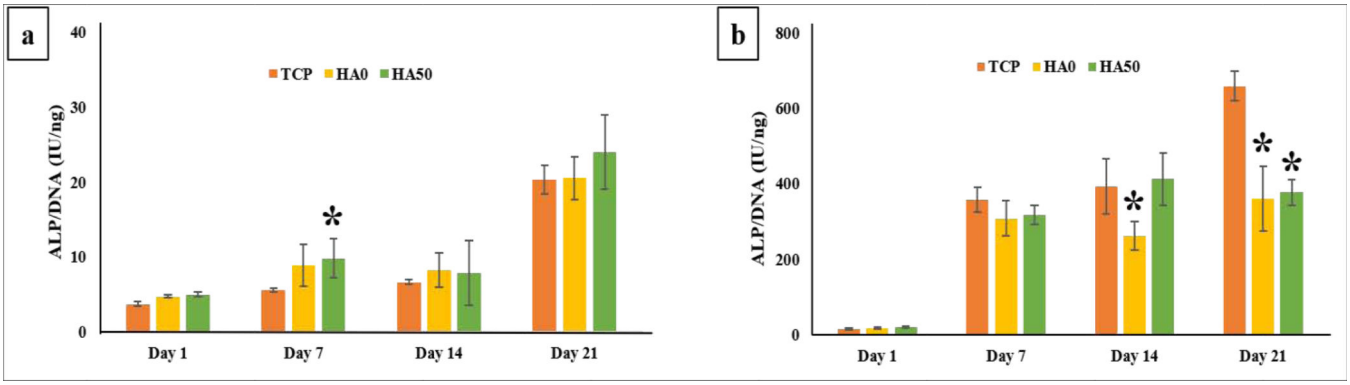

Fig. 9:

ALP activity by W-20-17 cells in regular medium (a) and 25ng/ml BMP-2 medium (b). HA0 and HA50 membranes were evaluated for their osteogenic potential and compared with controls. Each value represents the mean ± SD (n= 4 per each group) *represents significant difference between membrane group and control. $p<0.05$ was considered to be statistically significant.

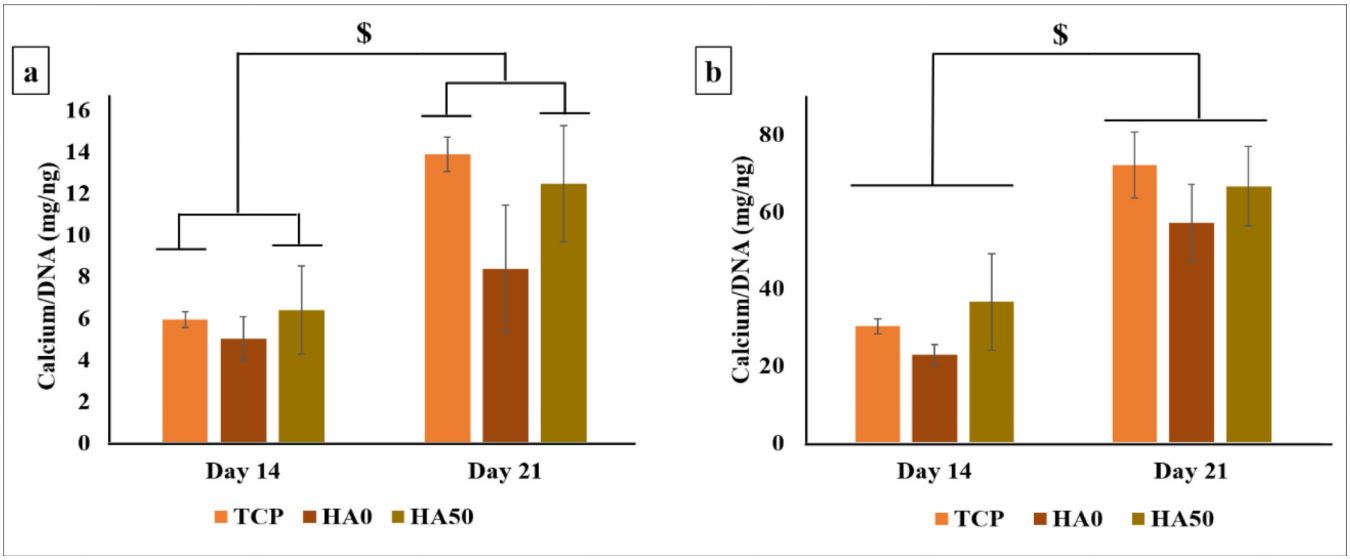

Fig. 10:

Calcium assay to quantify the amount of calcium deposited on W-20-17 cells in regular osteogenic media (a) and 25ng/ml BMP-2 supplemented osteogenic media (b). HA0 and HA50 membranes were evaluated for their osteogenic potential and compared with controls. Each value represents the mean ± SD (n= 4 per each group). **$** represents significant difference between day 21 vs day 14 for corresponding groups. $p<0.05$ was considered to be statistically significant.

Table 1:

Water contact angle measurement of differently modified membranes. Each value represents mean ± standard deviation (n=4)

Membrane modification	Water contact angle (°)
AA	59.3 ± 8.2[a]
BA	73.3 ± 5.4[b]
HA	94.3 ± 8.5[c]
tBOC	119.3 ±17.4[d]

Superscripts indicate statistically different groups, $p<0.05$

Table 2:

Elemental analysis of original chitosan, as spun chitosan and modified chitosan.

	Elements	Original chitosan	As spun	tBOC	AA	BA	HA
Atomic wt%	C	39.8	33.38	42.3	42.11	48	56.56
	H	6.99	5.42	6.93	6.84	7.07	7.87
	N	6.95	4.68	5.7	5.58	5.27	4.12
	F	0	14.5	0	0	0	0
Atomic number ratio	C/N	6.68[a]	8.32	8.65	8.80	10.62	16.01
DM			0.82[b]	0.40	1.06	0.99	1.56

[a] theoretical $n_0(C)/n_0(N)$ is 6.58 for DDA 71% chitosan.

[b] as spun membrane includes TFA salt.

Table 3:

Percentage cumulative release of SMV from thick membranes after 28 and 91 days of elution.

	After 28 days				After 91 days			
	500μg	***250μg***	***100μg***	***50μg***	***500μg***	***250μg***	***100μg***	***50μg***
AA	17.8 ± 3.2	29.5 ± 2.4	48.2 ± 4.8	73 ± 33.2	32.9 ± 5.5	42.5 ± 4.1	53.6 ± 4.8	104.6 ± 14
BA	8.5 ± 1.6	11.7 ± 2.0	21.1 ± 0.7	45.0 ± 3.5	12.3 ± 1.8	16.8 ± 1.7	29.6 ± 1.4	58.5 ± 4.3
HA	4.8 ± 0.8	8.9 ± 0.5	19.9 ± 0.6	43.0 ± 3.5	6.8 ± 1.0	12.0 ± 0.6	26.8 ± 1.3	56.5 ± 3.3
tBOC	15.8 ±1.3	29.4 ± 3.9	53.9 ± 9.8	88.8 ± 17.7	27.8 ± 5.2	43.7 ± 10.7	60.2 ± 10.9	102.9± 9.3

Table 4:

Estimated Hansen Solubility Parameters for SMV, hydrolyzed SMV and chitosan with different modifications

	δ_D	δ_P	δ_H	$\Delta\delta_I^2$ (MPa$^{0.5}$)
Chitosan	17.77	11.29	15.16	25.94
AA-Chitosan	17.40	9.58	11.33	22.87
BA-Chitosan	17.00	8.67	9.71	21.41
HA-Chitosan	16.89	8.05	9.70	21.07
tBOC-Chitosan	17.21	11.74	12.14	24.11
SMV	16.80	0.42	4.26	17.34
Hydrolyzed SMV	16.99	3.26	7.10	18.70

Table 5:

Hansen solubility differences and polymer-drug interaction parameters at 310K (37°)

	$A_{1,2}$		$\chi_{1,2}$(310K)	
	SMV	***Hydrolyzed SMV***	***SMV***	***Hydrolyzed SMV***
Chitosan	60.19	32.97	9.55	5.19
AA-Chitosan	33.85	14.64	5.37	2.31
BA-Chitosan	24.46	9.01	3.88	1.42
HA-Chitosan	21.96	7.44	3.49	1.17
tBOC-Chitosan	47.73	24.38	7.58	3.84